# Probing Tyrosine Nitration with a Small Tb<sup>III</sup>-Metallopeptide

Rosalía Sánchez-Fernández,[a] Agustín Sánchez-Temprano,[a] David Esteban-Gómez,[a] and Elena Pazos*[a]

Tyrosine nitration, a post-translational modification (PTM) that takes place under nitrosative stress conditions, occurs through a non-enzymatic peroxynitrite-mediated reaction. Although protein nitration has long been considered an irreversible PTM involved in nitrosative stress-associated diseases, it has also been suggested to be a regulatory mechanism of signal transduction. Therefore, the development of tools that help to understand this protein modification is of great interest. Herein, we explore a Tb<sup>III</sup>-chelating metallopeptide to monitor tyrosine nitration. The luminescence of this probe decreases significantly between its non-nitrated and nitrated states, and this reduction in the luminescence intensity is directly related to the degree of tyrosine nitration after treatment with peroxynitrite. Remarkably, the luminescence intensity changes after nitration are not affected in the presence of complex biological media, which makes it a promising tool for understanding this protein modification.

## Introduction

Many proteins undergo a variety of covalent modifications, known as post-translational modifications (PTM), after being synthesized by the ribosomes. These modifications are usually enzymatic, such as phosphorylation, which is a highly important reversible mechanism involved in most cell-signaling pathways. Other types of PTMs, such as tyrosine nitration, cysteine S-nitrosylation, and glutathionylation, occur as consequence of oxidative and nitrosative stress.[1,2] Tyrosine nitration has been proposed to occur non-enzymatically in biological systems, through a stepwise pathway with peroxynitrite-derived radicals that promote the oxidation of tyrosine to its corresponding tyrosyl radical, which upon combination with nitrogen dioxide radical ($^\bullet NO_2$), also produced through the decay pathways of $ONOO^-$, leads to the formation of 3-nitrotyrosine (3-nTyr).[3–5]

Although low levels of protein tyrosine nitration are detected under basal conditions, there is a significant increase in nitroxidative stress-associated diseases, such as neurodegenerative, inflammatory and cardiovascular conditions.[6,7] In these circumstances, nitration of protein tyrosine residues can induce different effects on protein function.[1,3,4,6,7] For example, nitration of glutathione reductase residues Tyr106 and Tyr114 promotes a loss of function by reducing its activity due to the decreased binding affinity for its substrate.[8,9] The opposite effect is observed in cytochrome $c$,[10] protein kinase Cε,[11] or α-synuclein,[12] among others, which after nitration would show a new or increased function associated with a significant biological effect. In the case of α-synuclein, nitrated monomers and dimers have been described to accelerate the rate of fibril formation, and thus may induce the formation of intracytoplasmic inclusions characteristic of Parkinson's disease and other synucleinopathies. However, even though protein nitration has long been considered as an irreversible PTM, it has also been suggested that it could be a regulatory mechanism of signal transduction,[13] similar to protein phosphorylation/dephosphorylation, because of the precedents reporting the reversibility of this protein modification by showing denitrase activity.[14–19] Usually, protein tyrosine nitration/denitration has been identified by using anti-tyrosine antibodies or mass-spectrometry.[14,16–19] Nevertheless, these methods have some limitations, for example, not suitable for live-cellular imaging. An interesting alternative is the use of luminescent probes to study the species involved in this protein modification.

In contrast to organic fluorophores, luminescent lanthanide ion complexes show unique photophysical properties that make them very interesting for biosensing/bioimaging, such as narrow emission bands, long lifetimes, which offer the possibility of removing the autofluorescence signal of biological media by carrying out time-resolved luminescence assays, and large Stokes shifts that facilitate the elimination of self-quenching processes.[20,21] Indeed, there are precedents of lanthanide-based probes designed to detect $ONOO^-$ using different sensing mechanisms.[22–25] However, developing sensors for the specific detection of the end nitrated/denitrated products would be a valuable tool for understanding this PTM.

In this context, peptide-based luminescent probes are very appealing because they can easily mimic the natural substrates involved in nitration and denitration processes. Zondlo's group has reported an encoded protein-based probe that is responsive to tyrosine nitration, providing a novel approach to understanding this protein modification.[25] However, this turn-

**ChemBioChem**

Research Article
doi.org/10.1002/cbic.202300072

**Chemistry
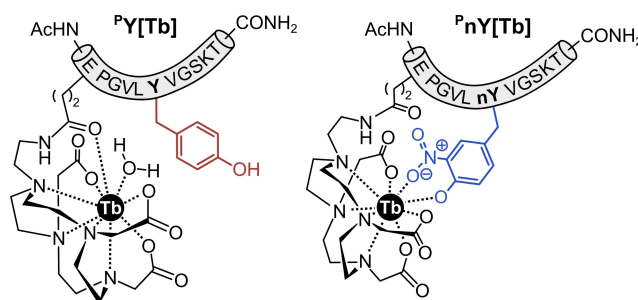Europe**
European Chemical
Societies Publishing

off probe is based on an EF-hand metal-binding motif with moderate $Tb^{III}$ binding affinities on its nitrated/non-nitrated states (micromolar range), and shows only a modest decrease in the luminescence response, roughly three times, after nitration. Herein, we describe a novel strategy for monitoring nitration states using a synthetic $Tb^{III}$ peptide complex that exhibits a large luminescence change, approximately 40-fold, between its nitrated and non-nitrated states. Importantly, its luminescence decreases after treatment with $ONOO^-$ and the difference in luminescence intensity between the nitrated and non-nitrated states it is not affected by the presence of complex biological media.



**Scheme 1.** Peptide sequences and proposed coordination of $Tb^{III}$ in **$^PY[Tb]$** and **$^PnY[Tb]$**.

## Results and Discussion

As starting point for our design, we selected the peptide sequence from Gly36 to Thr44 of α-synuclein (GVLYVGSKT) that has been found nitrated both *in vitro*[26] and *in vivo*.[27] At the *N*-terminus of this peptide, we included a Glu residue and attached to its side chain a DO3A macrocyclic derivative, which is known to form thermodynamically and kinetically stable complexes with lanthanide ions.[28–30] We also added a Pro residue between the Glu and the Gly residues to induce a β-turn that should favor the organization of the $Tb^{III}$ complex closer to the Tyr antenna (**$^PY[Tb]$**, Scheme 1).[31–35] Thus, our sensing mechanism relies on the irreversible modification of the Tyr antenna after reacting with $ONOO^-$ yielding **$^PnY[Tb]$**,[21] where the excited 3-nTyr residue deactivates in a femtosecond timescale through a conical intersection,[36] therefore switching off the luminescence of the metallopeptide.

Peptides **$^PY$** and **$^PnY$** were synthesized by solid phase peptide synthesis following standard Fmoc/*t*Bu protocols. The Glu residue was introduced in the peptide sequences protected on its side chain with an allyl group, which was selectively removed by Pd catalysis,[32] and then the DO3A ethylamino derivative **3** was coupled to the deprotected carboxylic acid side chains of **$^PY$** and **$^PnY$**. The resulting peptides **$^PY$** and **$^PnY$** were deprotected and cleaved from the solid support and purified by reversed-phase HPLC.

As expected, the appearance of the characteristic emission bands of $Tb^{III}$ ions at 488, 544, 586 and 620 nm (for the

transitions $^5D_4\rightarrow^7F_J$, $J=6$, 5, 4, 3) after excitation of the Tyr antenna at 260 nm, confirmed that **$^PY$** is able to coordinate this metal ion when incubated in HEPES buffer (10 mM HEPES, 100 mM NaCl, pH 7.5) in an equimolar mixture with $TbCl_3$ (Figure 1A and Figure S5 in the Supporting Information). On the other hand, the luminescence spectrum of the equimolar mixture of the nitrated peptide **$^PnY$** with $TbCl_3$ showed a significant decrease of the $Tb^{III}$ emission ($\approx 40$ times). Additionally, ESI-MS spectra of both **$^PY$** and **$^PnY$** mixtures with $TbCl_3$ confirmed the formation of the corresponding terbium peptide complexes, **$^PY[Tb]$** and **$^PnY[Tb]$** (Figure S3), thus demonstrating that the decrease in the emission intensity of the **$^PnY$** and $TbCl_3$ mixture is due to the 3-nTyr chromophore and not to a difference in binding affinity of the peptide for the $Tb^{III}$ ion.

We measured the luminescence lifetime of **$^PY[Tb]$** and **$^PnY[Tb]$** in water and $D_2O$ and fitted the emission decays to a single exponential (Figure S6 and Table S1). **$^PY[Tb]$** showed a long lifetime in water (1.54 ms) that increased in $D_2O$ (3.23 ms). These lifetime values allowed us to calculate the inner-sphere water molecules coordinated to the metal ion ($q$),[37] which for **$^PY[Tb]$** was estimated to be $q\approx 1.4$. This value is in good agreement with those reported for similar DO3A-based lanthanide complexes and is compatible with the coordination of the Glu side chain carbonyl to the metal center (Scheme 1).[32,38] The lifetime values obtained for **$^PnY[Tb]$** (1.61 ms in water and 2.10 ms in $D_2O$) allowed us to estimate the number of water

Elena Pazos obtained her PhD in 2012 from the Universidade de Santiago de Compostela under the supervision of Prof. José L. Mascareñas and Prof. M. Eugenio Vázquez. In 2012 she joined the group of Prof. Samuel I. Stupp at Northwestern University. She moved to Medcom Advance in 2014, and from December 2015 worked in the group of Prof. Ramón A. Álvarez-Puebla at Centre Tecnològic de la Química. In July 2017, she joined the Universidade da Coruña, where she currently holds a Ramón y Cajal contract. Her research group focuses on the development of new peptide-based materials and luminescent probes.
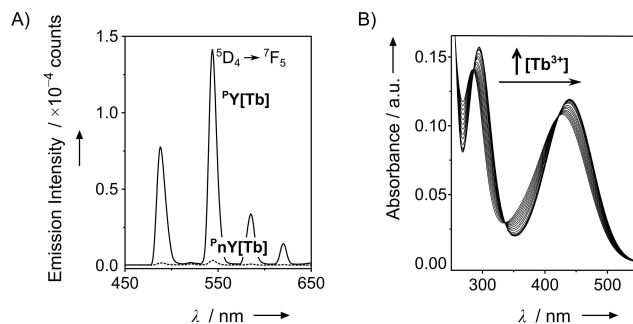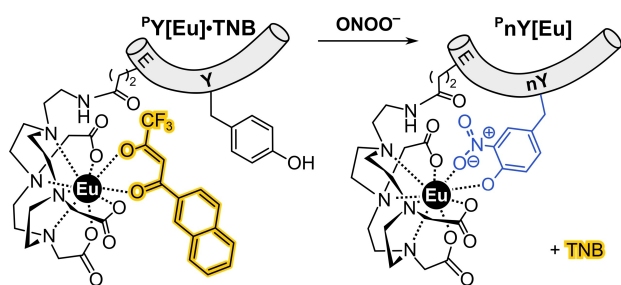
**Figure 1.** A) Luminescence spectra of 10 μM **$^PY[Tb]$** (solid line) and **$^PnY[Tb]$** (dashed line) in 10 mM HEPES, 100 mM NaCl, pH 7.5, $\lambda_{ex}=260$ nm. B) UV-vis titration of 30 μM **$^PnY$** in 10 mM HEPES, 100 mM NaCl, pH 7.5, with increasing concentrations of $TbCl_3$.

**ChemBioChem**

Research Article
doi.org/10.1002/cbic.202300072

**Chemistry
Europe**
European Chemical
Societies Publishing

molecules coordinated to the metal center, $q \approx 0.4$, suggesting the displacement of a water molecule from the coordination sphere of the $Tb^{III}$ ion by the 3-nTyr residue. The electron-withdrawing nitro group reduces the $pK_a$ value of the Tyr residue to $\approx 6.74$,[39] making it a better donor for the metal center and thus facilitating its coordination to the $Tb^{III}$ ion as a bidentate ligand (Scheme 1).[25,40] The UV-vis titration of $^P$nY in HEPES buffer with increasing concentrations of $TbCl_3$ showed an increase and a red-shift of the 3-nTyr bands at 284 and 428 nm, associated to the anionic form of the 3-nTyr residue,[39] up to the addition of 1 equivalent of $Tb^{III}$ (Figures 1B and S9), also indicating the coordination of the chromophore 3-nTyr to the metal center.

To better understand the coordination sphere of $^P$nY[Tb] we studied its $Eu^{III}$ analogs. Peptides $^P$Y and $^P$nY in HEPES buffer were mixed with 1 equivalent of $EuCl_3$ and the mixtures were analyzed by ESI-MS, showing the formation of the corresponding $^P$Y[Eu] and $^P$nY[Eu] complexes (Figure S4). As the solutions of $^P$Y[Eu] and $^P$nY[Eu] in HEPES buffer were not luminescent, and considering that the DO3A derivative **3** does not satisfy all the available coordination positions of the metal center, as observed for $^P$Y[Tb], we decided to use an external coordinating antenna to fulfill the coordination sphere of $Eu^{III}$. For this purpose, we selected the bidentate ligand 4,4,4-trifluoro-1-(2-naphthyl)-1,3-butanedione (**TNB**), which has been previously reported to efficiently coordinate and sensitize DO3A-based macrocyclic $Eu^{III}$ complexes (Scheme 2).[32,41] The luminescence titration of a 2.5 μM $^P$Y[Eu] solution in HEPES buffer with increasing concentrations of **TNB** showed the increase of the $Eu^{III}$ characteristic emission bands at 595, 615, 654 and 691 nm (for the transitions $^5D_0 \rightarrow {}^7F_J$, $J = 1$, 2, 3, 4), corroborating the formation of the $^P$Y[Eu]·**TNB** complex with a $K_{D1} \approx 2.1$ μM (Figures 2A and S10). We evaluated the stability of the $^P$Y[Eu]·**TNB** complex in HEPES buffer and observed that the luminescence of the complex does not change for at least 30 h (Figure S11). $^P$Y[Eu]·**TNB** has a shorter lifetime in water than $^P$Y[Tb], which slightly increases in $D_2O$ (0.87 and 1.16 ms, respectively, Figure S12 and Table S2). These values allowed us to calculate the number of water molecules coordinated to $Eu^{III}$,[42] which turned out to be $q \approx 0$, thus confirming the coordination of the external antenna to the $Eu^{III}$ ion. As expected, the luminescence spectrum of a 10 μM $^P$nY[Eu] and 10 μM **TNB** mixture in HEPES buffer showed a much weaker
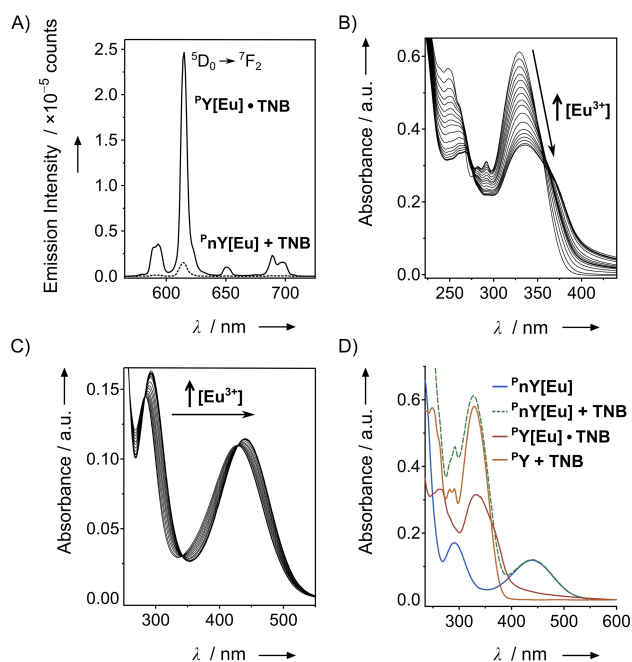


**Figure 2.** A) Luminescence spectra of 10 μM $^P$Y[Eu]·**TNB** (solid line) and a 10 μM $^P$nY[Eu] and 10 μM **TNB** mixture (dashed line) in 10 mM HEPES, 100 mM NaCl, pH 7.5, $\lambda_{ex} = 260$ nm. B) UV-vis titration of a 30 μM $^P$Y[Eu] and 30 μM **TNB** mixture in 10 mM HEPES, 100 mM NaCl, pH 7.5, with increasing concentrations of $TbCl_3$. C) UV-vis titration of 30 μM $^P$nY in 10 mM HEPES, 100 mM NaCl, pH 7.5, with increasing concentrations of $EuCl_3$. D) UV-vis spectra of a 30 μM $^P$Y[Eu]·**TNB** solution (solid red line), a 30 μM $^P$nY[Eu] solution (solid blue line), a 30 μM $^P$Y and 30 μM **TNB** mixture (solid orange line), and a 30 μM $^P$nY[Eu] and 30 μM **TNB** mixture (dashed green line) in 10 mM HEPES, 100 mM NaCl, pH 7.5.

emission intensity, of about 20 times, compared to $^P$Y[Eu]·**TNB** (Figure 2A). Furthermore, the lifetime measurements of $^P$nY[Eu] in the presence of **TNB**, both in water and $D_2O$ (0.70 and 0.84 ms, respectively) could be fitted to a two-phase exponential decay, one of them associated to the free **TNB** in solution and the other one to $^P$nY[Eu] (Figure S12 and Table S2). These data allowed us to estimate the number of water molecules coordinated to the $Eu^{III}$ complex, which resulted to be $q \approx 0$, confirming the displacement of the **TNB** antenna from the $Eu^{III}$ coordination sphere by the 3-nTyr residue, and thus the decrease in the luminescence intensity. These results were further corroborated by UV-vis spectroscopy. The UV-vis titration of a 30 μM $^P$Y and 30 μM **TNB** mixture in HEPES buffer showed a decrease, a redshift, and a broadening of the **TNB** absorption band at 330 nm[41] with increasing concentrations of $EuCl_3$ (Figures 2B and S13), clearly indicating the coordination of the antenna to the metal ion and the formation of the $^P$Y[Eu]·**TNB** complex.

A similar effect was observed when we recorded the UV-vis spectra of a 30 μM $^P$nY solution with increasing concentrations of $EuCl_3$. As shown in Figures 2C and S14, and as observed for $^P$nY[Tb], the addition of 1 equivalent of $EuCl_3$ promoted the redshift of the 3-nTyr absorption bands, pointing towards the formation of $^P$nY[Eu], where the $Eu^{III}$ ion is coordinated by the 3-nTyr residue. When we compared the UV-vis spectra of 30 μM



**Scheme 2.** Proposed sensing mechanism for the detection of tyrosine nitration by displacement of the external antenna from the $Eu^{III}$ coordination sphere by the 3-nTyr residue after reaction of $^P$Y[Eu]·**TNB** with ONOO⁻.

**ChemBioChem**

Research Article
doi.org/10.1002/cbic.202300072

**Chemistry
Europe**
European Chemical
Societies Publishing

solutions of **PY**, **PY[Eu]**, and **PnY[Eu]** in the presence of equimolar amounts of **TNB** with a **PnY[Eu]** solution in HEPES buffer (Figure 2D and S15), we observed that the absorption band at 330 nm of the **PnY[Eu]** and **TNB** mixture spectrum, characteristic of free **TNB** in solution, pretty much overlays with the corresponding band of the **PY** and **TNB** mixture spectrum, and not with the experimental bands recorded for the **PY[Eu]·TNB** complex, where the **TNB** is coordinated to the Eu$^{III}$ ion. In a similar way, the absorption band at 428 nm, characteristic of the anionic form of the 3-nTyr residue, is redshifted almost 10 nm in the **PnY[Eu]** and **TNB** mixture spectrum, overlapping with the corresponding band of the **PnY[Eu]** complex spectrum. All together, these results demonstrate that the anionic form of the 3-nTyr residue of the **PnY[Tb]** and **PnY[Eu]** complexes is coordinated to the metal ions, satisfying all their coordination positions.

To evaluate the potential luminescent response of the **PY[Tb]** probe to protein nitration, we performed a control experiment in which we recorded the luminescent spectra of mixtures with different **PY[Tb]** and **PnY[Tb]** ratios. As expected, we observed a lineal response in the decrease of the luminescence intensity with increasing amounts of **PnY[Tb]** (Figure S16). We then assessed the sensitivity of **PY[Tb]** and **PY[Eu]·TNB** towards protein nitration. Both probes were incubated in the absence and with different concentrations of ONOO⁻, and the conversion to their nitrated states, **PnY[Tb]** and **PnY[Eu]**, was analyzed by their luminescent response and confirmed by reversed-phase HPLC. **PY[Tb]** exhibited approximately a 14% and a 36% decrease in the luminescence intensity after treatment with 5 and 10 equiv. of ONOO⁻, respectively, which are in agreement with the amounts of nitrated probe quantified by HPLC (Figure 3). However, although **PY[Eu]·TNB** also showed a decrease of the luminescence with ONOO⁻, the reduction of the luminescence intensity was lower than expected according to the extent of nitration determined by HPLC, probably due to a competing process between **PY[Eu]·TNB** and some unidentified subproduct of the reaction. Importantly, when we registered the luminescence spectra of **PY[Tb]** and the nitrated mixtures in a complex medium, as it is in the presence of cell extracts (total protein concentration ≈63 μg mL⁻¹), we did not observe a significant effect on the luminescent signal of **PY[Tb]** and the luminescent decrease in the nitrated mixture corresponded with the degree of nitration of the probe (Figure S19). Therefore, these experiments demonstrate the advantages of using luminescent lanthanide probes, which allow to remove the intrinsic background signal of complex biological media as shown in Figure S20.

## Conclusion

We have developed a small Tb$^{III}$ metallopeptide whose luminescence intensity is significantly quenched when the Tyr antenna in the peptide sequence is nitrated. We have demonstrated that the luminescence decrease of the probe is correlated with the degree of tyrosine nitration after being exposed to different concentrations of ONOO⁻. Importantly, the luminescence response of the probe is not affected by complex biological media. Therefore, the probe developed herein provides a new tool to understand protein tyrosine nitration in cell lysates and study if this modification could actually be a regulatory mechanism of signal transduction, as has been suggested in the literature. Future work in our lab will address some of the current limitations of the probe, streamlining the calibration process and extending the excitation wavelength for cellular imaging.

## Experimental Section

**General**: Amino acid derivatives, as Fmoc amino acids with the standard side-chain-protecting scheme, and coupling agents were purchased from Iris Biotech GmbH and NovaBioChem. C-terminal amide peptides were synthesized on a 0.1 mmol scale using a 0.41 mmol/g loading H-Rink amide ChemMatrix resin from Merck. DO3AtBu ester **1**, precursor of the chelating macrocycle **3**, was purchased from Activate Scientific. Protease inhibitor cocktail was purchased from Thermo Scientific. All other chemicals were purchased from Fisher Scientific and Merck. All solvents were synthesis grade, except for DMF, DIEA, and TFA that were peptide synthesis grade. Water was purified using a Milli-Q system (Millipore).

**Synthesis of DO3AtBu-NEtNH₂ (3)**: The chelating macrocycle **3** was synthesized according to the procedures described in the literature (see the Supporting Information).[43]

**Peptide synthesis**: Peptides were synthesized using standard Fmoc solid-phase peptide synthesis procedures using a PS3 automatic peptide synthesizer from Protein Technologies Inc. Amino acid couplings were conducted using a fourfold excess and HBTU (4 equiv.) as activating agent. Each amino acid was activated for 2 min in DIEA/DMF (6 equiv.) before being added onto the resin. Peptide bond-forming couplings were carried out for 30 min. After the deprotection of the Fmoc group by treating the resin with a 20% 4-methylpiperidine (4-MP) solution in DMF for 15 min, the final peptide sequences were acetylated by treatment of the resin with a mixture of Ac₂O (12 equiv.) and DIEA/DMF (0.195 M,
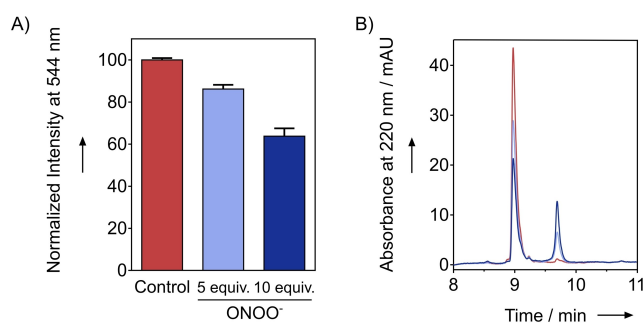


**Figure 3.** A) Normalized emission intensity at 544 nm of a 2.5 μM **PY[Tb]** solution (control sample) and 2.5 μM solutions of the corresponding reaction mixtures of **PY[Tb]** with 5 and 10 equiv. of ONOO⁻ in 10 mM HEPES, 100 mM NaCl, pH 7.5, $\lambda_{ex} = 260$ nm. B) HPLC chromatograms at 220 nm of the **PY** control sample (red) and the reaction mixtures of **PY** with 5 (light purple) and 10 equiv. (dark blue) of ONOO⁻, where the peak at $t_R \approx 9.0$ min corresponds to **PY** and the peak at $t_R \approx 9.7$ min corresponds to **PnY**. Considering the integrated peak areas, the **PY** conversion to **PnY** was estimated to be 15.5% and 28.0% with 5 and 10 equiv. of ONOO⁻, respectively.

**ChemBioChem**

Research Article
doi.org/10.1002/cbic.202300072

**Chemistry
Europe**
European Chemical
Societies Publishing

10 equiv.) for 45 min. After filtration, the resins were washed with DMF and $CH_2Cl_2$. The side chain of the N-terminal Glu(All) residue was selectively deprotected by treating the resin with a mixture of $Pd(OAc)_2$ (0.3 equiv.), $PPh_3$ (1.5 equiv.), N-methylmorpholine (NMM, 10 equiv.), and $PhSiH_3$ (10 equiv.) in $CH_2Cl_2$ overnight. After filtration, the resulting resin was washed with DMF (2×5 min), N,N-diethyldithiocarbamate (DEDTC, 25 mg in 5 mL DMF, 10 min), and $CH_2Cl_2$ (2×5 min), and dried under a $N_2$ current. A solution of HBTU (1 equiv.) in DMF was mixed with DIEA/DMF (0.195 M, 4 equiv.) and the mixture was added to the resins (0.03 mmol) and mixed for 2 min before adding DO3AtBu-NEtNH$_2$ (**3**; 2 equiv.) over the resins. The mixture was left stirring under $N_2$ for 1 h. After filtration, the resins were washed with DMF and $CH_2Cl_2$. The cleavage/deprotection step was performed adding a TFA cleavage cocktail (2.5% $H_2O$, 2.5% triisopropysilane (TIS) and 95% TFA) to the resin-bound peptides, and the mixtures were left stirring for 5.5 h. After precipitation of the TFA filtrates in cold $Et_2O$, the peptides were dissolved in 1:1 MeCN/$H_2O$. The purification of the peptides was performed in an Agilent 1200 series using an Aeris semipreparative column from Phenomenex (peptide XB—C18 stationary phase, 5 μm, 100 Å pore size, 250×10 mm). The methods used for semi-preparative HPLC were 15→36.5% MeCN, 0.1% TFA/$H_2O$, 0.1% TFA over 16 min for **PY** and 15→35% MeCN, 0.1% TFA/$H_2O$, 0.1% TFA over 24 min for **PnY**. Reversed-phase HPLC and electrospray ionization mass spectrometry (ESI/MS) analyses were performed using a liquid chromatograph mass spectrometer system, Thermo Scientific UltiMate 3000 connected to a photo-diode array detector and a single quadrupole mass spectrometer Thermo Scientific MSQ Plus or a Bruker Elute UHPLC connected to a high-resolution TIMS-QTOF Bruker Daltonics timsTOF Pro with a Bruker Daltonics CaptiveSpray ion source, using an Aeris analytical column (peptide XB—C18 stationary phase, 3.6 μm, 100 Å pore size, 150×2.1 mm) or a Luna analytical column (Omega Polar C18 stationary phase, 3 μm, 100 Å pore size, 150×2.1 mm), both from Phenomenex. The standard method used for analytical HPLC was 5→95% MeCN, 0.04% TFA/$H_2O$, 0.04% TFA over 23 min.

**PY**: HPLC: retention time $(t_R)$ = 10.5 min. ESI-MS (m/z) calculated for $C_{70}H_{116}N_{18}O_{22}$: 1561.8584 $[MH]^+$; found 781.4329 $[M+2H]^{2+}$, 521.2917 $[M+3H]^{3+}$ (1.7 mg, 4% yield for a 0.03 mmol scale).

**PnY**: HPLC: $t_R$ = 11.2 min. ESI-MS (m/z) calculated for $C_{70}H_{115}N_{19}O_{24}$: 1606.8435 $[MH]^+$; found 803.9255 $[M+2H]^{2+}$, 536.2861 $[M+3H]^{3+}$ (1.8 mg, 4% yield for a 0.03 mmol scale).

**Luminescence assays**: Time-gated emission measurements were made with a FluoroMax Plus-P Spectrofluorometer from Horiba Scientific equipped with an R928P photon counting emission detector, in the phosphorescence mode using a xenon flash lamp. All measurements were made with a Hellma Semi-Micro cuvette (114F-10-40, 10 mm light path) at 25°C, using the following settings: excitation wavelength 260 nm; excitation slit width 10.0 nm, emission slit width 3.0 nm; increment 2.0 nm; time between flashes 0.061 s; initial delay 0.2 ms; sample window 0.02 s; flash count 0.01 s; HV detector voltage 950 V. The emission spectra for Tb$^{III}$ and Eu$^{III}$ complexes were recorded from 450 to 600 nm and 550 to 750 nm, respectively.

**Lifetime experiments**: Lifetime experiments were measured on the same instrument and cuvette as for the luminescence assays, using the following settings: excitation wavelength 260 nm; emission wavelength 544 or 615 nm for Tb$^{III}$ and Eu$^{III}$ complexes, respectively; excitation and emission slit width 6.0 nm; measurement range 22.0 ms; HV detector voltage 950 V; peak preset 10000 counts. The measurements were recorded using a 475 nm long-pass filter to avoid interference from harmonic doubling.

The decay data of the emission intensity were fit to a single or double exponential decay based on the function [Eq. (1)]:

$$I(t) = \sum_{i=1}^{2} A_i \exp(-t/\tau_i) \qquad (1)$$

where $I(t)$ is the intensity of phosphorescence at time $t$ after the excitation pulse, $A_i$ is the pre-exponential factor, and $\tau$ is the luminescence lifetime. By measuring the luminescence decay ($\tau$) in both $H_2O$ and $D_2O$ solutions, the number of water molecules ($q$) can be estimated from Equation (2):

$$q = A\left(1/\tau_{H_2O} - 1/\tau_{D_2O} - B + Cn_{O=CNH}\right) \qquad (2)$$

where $A$ = 5 ms, $B$ = 0.06 ms$^{-1}$, and $C$ = 0 for Tb$^{III}$,[32,37] and $A$ = 1.11 ms, $B$ = 0.3 ms$^{-1}$, $C$ = 0.075 ms$^{-1}$ and $n_{O=CNH}$ = 1 (the number of amide N—H oscillators) for Eu$^{III}$.[37,42]

**UV-vis spectroscopy**: UV measurements were performed on a Jasco V-750 Spectrometer, using a standard 10 mm light pass Hellma Semi-Micro cuvette (114-10-40) at 25°C, using the following settings: UV/Vis bandwidth 5.0 nm, UV/Vis response 0.06 s; data interval 0.5 nm; scan mode continuous, scan speed 200 nm/min. Concentrations were determined using the following molar extinction coefficients: 1405 M$^{-1}$cm$^{-1}$ for Tyr at 274 nm in 0.1 M phosphate buffer pH 7.0,[44] 2200 M$^{-1}$cm$^{-1}$ for 3-nTyr at 381 nm in water,[39] and 1670 M$^{-1}$cm$^{-1}$ for ONOO$^-$ at 302 nm in 1.2 M NaOH.[45]

**Preparation of cell lysates**: Asynchronously growing HEK293T cells were lysed in HEPES lysis buffer (50 mM HEPES, 150 mM NaCl, 10 mM EDTA, 1% NP40 and protease inhibitor cocktail, pH 7.4). Lysates were cleared by centrifugation and protein content in the supernatant was measured by the Bradford method.[46] Protein extracts were stored at −20°C until used in the assays.

**PY nitration experiments**: **PY** nitration experiments were conducted following procedures described in the literature.[25] To 250 μL of a 100 μM solution of **PY** in nitration buffer (100 mM $K_2HPO_4$, 25 mM NaHCO$_3$, 0.2 mM EDTA, pH 7.5), 1.65 μL (5 equiv.) or 3.3 μL (10 equiv.) of a 74.4 mM stock solution of ONOO$^-$ were rapidly added, followed by the addition of 1 or 2 μL of 1 M HCl, respectively, and the final solution was subjected to vigorous vortexing for 60 s in darkness. Afterwards, reactions were quenched by adding 5 μL of a 100 mM solution of dithiothreitol, DTT, followed by vigorous vortexing for 5 min. Control samples were prepared by adding ONOO$^-$ and DTT to the nitration buffer before the addition of **PY**. Sample mixtures were eluted by reversed-phase HPLC, in order to remove salts and nitration byproducts (Agilent 1200 series using a Poroshell 120 EC—C18 analytical column, 4 μm, 120 Å pore size, 100×4.6 mm from Agilent), and the eluted fractions were collected and freeze-dried. Samples were dissolved in 260 μL of HEPES buffer and analyzed by RP-HPLC and UV-vis (see the Supporting Information). Peptide concentrations were determined by the extrapolation of the integrated peak areas from calibration curves of **PY** and **PnY** (see the Supporting Information). 1 mL of control or reaction mixtures solutions were prepared in HEPES buffer with a 2.5 μM total peptide concentration. To these solutions, TbCl$_3$ or EuCl$_3$ and **TNB** were added up to a 2.5 μM concentration and the final solutions were shaken for 2 h. The **PY** conversion to **PnY** was calculated by considering the **PnY** concentration obtained in the reaction divided by the total peptide concentration in the mixtures. Time-gated emission measurements were made in a Varian Cary Eclipse Fluorescence Spectrophotometer, in the phosphorescence mode with a Hellma Semi-Micro cuvette (114F-10-40, 10 mm light path) at room temperature, using the following settings: excitation wavelength 260 nm; excitation slit width

**ChemBioChem**

Research Article
doi.org/10.1002/cbic.202300072

**Chemistry Europe**
European Chemical
Societies Publishing

## Acknowledgements

## Conflict of Interests

The authors declare no conflict of interest.

## Data Availability Statement

The data that support the findings of this study are available from the corresponding author upon reasonable request.

[1] L. H. Jones, *Chem. Biol.* **2012**, *19*, 1086–1092.
[2] N. R. Jayakumari, A. C. Reghuvaran, R. S. Rajendran, V. V. Pillai, J. Karunakaran, H. V. Sreelatha, S. Gopala, *Nitric Oxide* **2014**, *43*, 35–44.
[3] R. Radi, *Proc. Natl. Acad. Sci. USA* **2004**, *101*, 4003–4008.
[4] R. Radi, *Acc. Chem. Res.* **2013**, *46*, 550–559.
[5] G. Ferrer-Sueta, N. Campolo, M. Trujillo, S. Bartesaghi, S. Carballal, N. Romero, B. Alvarez, R. Radi, *Chem. Rev.* **2018**, *118*, 1338–1408.
[6] J. M. Souza, G. Peluffo, R. Radi, *Free Radical Biol. Med.* **2008**, *45*, 357–366.
[7] S. A. B. Greenacre, H. Ischiropoulos, *Free Radical Res.* **2001**, *34*, 541–581.
[8] D. Francescutti, J. Baldwin, L. Lee, B. Mutus, *Protein Eng.* **1996**, *9*, 189–194.
[9] S. N. Savvides, M. Scheiwein, C. C. Böhme, G. E. Arteel, P. A. Karplus, K. Becker, R. Heiner Schirmer, *J. Biol. Chem.* **2002**, *277*, 2779–2784.
[10] A. M. Cassina, R. Hodara, J. M. Souza, L. Thomson, L. Castro, H. Ischiropoulos, B. A. Freeman, R. Radi, *J. Biol. Chem.* **2000**, *275*, 21409–21415.
[11] Z. Balafanova, R. Bolli, J. Zhang, Y. Zheng, J. M. Pass, A. Bhatnagar, X. L. Tang, O. Wang, E. Cardwell, P. Ping, *J. Biol. Chem.* **2002**, *277*, 15021–15027.
[12] R. Hodara, E. H. Norris, B. I. Giasson, A. J. Mishizen-Eberz, D. R. Lynch, V. M. Y. Lee, H. Ischiropoulos, *J. Biol. Chem.* **2004**, *279*, 47746–47753.
[13] V. A. Yakovlev, R. B. Mikkelsen, *J. Recept. Signal Transduction* **2010**, *30*, 420–429.
[14] Y. Kamisaki, K. Wada, K. Bian, B. Balabanli, K. Davis, E. Martin, F. Behbod, Y. C. Lee, F. Murad, *Proc. Natl. Acad. Sci. USA* **1998**, *95*, 11584–11589.
[15] W. N. Kuo, R. N. Kanadia, V. P. Shanbhag, R. Toro, *Mol. Cell. Biochem.* **1999**, *201*, 11–16.
[16] Y. Irie, M. Saeki, Y. Kamisaki, E. Martin, F. Murad, *Proc. Natl. Acad. Sci. USA* **2003**, *100*, 5634–5639.
[17] H. S. Smallwood, N. M. Lourette, C. B. Boschek, D. J. Bigelow, R. D. Smith, L. Pa a-Toli, T. C. Squier, *Biochemistry* **2007**, *46*, 10498–10505.
[18] M. Kang, H. I. Akbarali, *FEBS Lett.* **2008**, *582*, 3033–3036.
[19] R. S. Deeb, T. Nuriel, C. Cheung, B. Summers, B. D. Lamon, S. S. Gross, D. P. Hajjar, *AJP Hear. Circ. Physiol.* **2013**, *305*, H687–H698.
[20] J.-C. G. Bünzli, *J. Lumin.* **2016**, *170*, 866–878.
[21] D. Parker, J. D. Fradgley, K. L. Wong, *Chem. Soc. Rev.* **2021**, *50*, 8193–8213.
[22] C. Song, Z. Ye, G. Wang, J. Yuan, Y. Guan, *Chem. Eur. J.* **2010**, *16*, 6464–6472.
[23] J. Wu, H. Liu, Y. Yang, H. Wang, M. Yang, *Opt. Mater.* **2018**, *77*, 170–177.
[24] C. Breen, R. Pal, M. R. J. Elsegood, S. J. Teat, F. Iza, K. Wende, B. R. Buckley, S. J. Butler, *Chem. Sci.* **2020**, *11*, 3164–3170.
[25] A. R. Urmey, N. J. Zondlo, *Biochemistry* **2019**, *58*, 2822–2833.
[26] J. M. Souza, B. I. Giasson, Q. Chen, V. M. Lee, H. Ischiropoulos, *J. Biol. Chem.* **2000**, *275*, 18344–18349.
[27] B. I. Giasson, J. E. Duda, I. V. Murray, Q. Chen, J. M. Souza, H. I. Hurtig, H. Ischiropoulos, J. Q. Trojanowski, V. M. Lee, *Science* **2000**, *290*, 985–989.
[28] R. M. Izatt, J. S. Bradshaw, K. Pawlak, R. L. Bruening, B. J. Tarbet, *Chem. Rev.* **1992**, *92*, 1261–1354.
[29] L. Tei, Z. Baranyai, L. Gaino, A. Forgács, A. Vágner, M. Botta, *Dalton Trans.* **2015**, *44*, 5467–5478.
[30] S. Gündüz, S. Vibhute, R. Botár, F. K. Kálmán, I. Tóth, G. Tircsó, M. Regueiro-Figueroa, D. Esteban-Gómez, C. Platas-Iglesias, G. Angelovski, *Inorg. Chem.* **2018**, *57*, 5973–5986.
[31] S. R. Raghothama, S. K. Awasthi, P. Balaram, *J. Chem. Soc. Perkin Trans. 2* **1998**, 137–143.
[32] E. Pazos, M. Goličnik, J. L. Mascareñas, M. Eugenio Vázquez, *Chem. Commun.* **2012**, *48*, 9534–9536.
[33] S. C. Zondlo, F. Gao, N. J. Zondlo, *J. Am. Chem. Soc.* **2010**, *132*, 5619–5621.
[34] A. M. Lipchik, L. L. Parker, *Anal. Chem.* **2013**, *85*, 2582–2588.
[35] J. Sumaoka, H. Akiba, M. Komiyama, *Int. J. Anal. Chem.* **2016**, *2016*, 3216523.
[36] L. Tang, C. Fang, *J. Phys. Chem. B* **2019**, *123*, 4915–4928.
[37] A. Beeby, I. M. Clarkson, R. S. Dickins, S. Faulkner, D. Parker, L. Royle, A. S. De Sousa, J. A. G. Williams, M. Woods, *J. Chem. Soc. Perkin Trans. 2* **1999**, *2*, 493–504.
[38] A. Congreve, D. Parker, E. Gianolio, M. Botta, *Dalton Trans.* **2004**, 1441–1445.
[39] V. De Filippis, R. Frasson, A. Fontana, *Protein Sci.* **2006**, *15*, 976–986.
[40] M. R. Bürgstein, P. W. Roesky, *Angew. Chem. Int. Ed.* **2000**, *39*, 549–551.
[41] J. P. Leonard, C. M. G. Dos Santos, S. E. Plush, T. McCabe, T. Gunnlaugsson, *Chem. Commun.* **2007**, 129–131.
[42] R. M. Supkowski, W. D. W. Horrocks, *Inorg. Chim. Acta* **2002**, *340*, 44–48.
[43] A. De La Reberdière, F. Lachaud, F. Chuburu, C. Cadiou, G. Lemercier, *Tetrahedron Lett.* **2012**, *53*, 6115–6118.
[44] *Handbook of Biochemistry and Molecular Biology* (Ed.: G. D. Fasman), CRC Press, Cleveland, **1976**, pp. 183–203.
[45] J. S. Beckman, J. Chen, H. Ischiropoulos, J. P. Crow, *Methods Enzymol.* **1994**, *233*, 229–240.
[46] N. J. Kruger, in, *Protein Protocols Handbook* (Ed.: J. M. Walker), Humana, Totowa, **2009**, pp. 17–24.